Lab on a Chip

Microfluidic particle zipper enables controlled loading of droplets with distinct particle types

Journal:	*Lab on a Chip*
Manuscript ID	LC-ART-04-2020-000339.R1
Article Type:	Paper
Date Submitted by the Author:	30-May-2020
Complete List of Authors:	Delley, Cyrille; University of California San Francisco, Bioengineering and Therapeutic Sciences Abate, Adam; University of California, San Francisco, Bioengineering and Therapeutic Sciences

Microfluidic particle zipper enables controlled loading of droplets with distinct particle types

Cyrille L. Delley[a], Adam R. Abate*[abc]

[a] Bioengineering and Therapeutic Sciences, University of California, San Francisco, San Francisco, CA 94158, USA.
[b] California Institute for Quantitative Biosciences, University of California San Francisco, San Francisco, CA 94158, USA
[c] Chan Zuckerberg Biohub, San Francisco, CA 94158, USA
*Corresponding Author, E-mail: adam@abatelab.org

Current encapsulation approaches control the number of particles encapsulated per droplet, but not the particle types; consequently, they are unable to generate droplets containing combinations of distinct particle types, limiting the reactions that can be performed. We describe a microfluidic particle zipper that allows the number and types of particles encapsulated in every droplet to be controlled. The approach exploits self-ordering to generate repeating particle patterns that allow controlled encapsulation in droplets. We use the method to combine barcode particles with gel encapsulated cells to profile multiple disease relevant genomic loci with single cell sequencing. Particle zippers can operate in series to generate complex particle compositions in droplets.

1. Introduction

In droplet microfluidic applications employing particles, it is optimal that each droplet receives an exact number of particles. For example, in single cell genomics, particles introduce barcode sequences to label DNA, RNA, and antibody-bound nucleic acids[1–4]; in these applications, it is optimal that each droplet be loaded with exactly one particle, ensuring that every cell is counted once and none are missed. In cell secretion assays involving particles, it is also optimal that each cell be paired with one particle, ensuring that all cells are analyzed and variation between droplets has to do with secretion and not particle counts[5]. When loading particles in droplets, random or ordered methods can be used. Random loading does not synchronize particle injection with droplet generation. This results in significant variation in which some droplets contain several particles and others are empty. By contrast, ordered loading synchronizes particles with droplets such that a controlled number is encapsulated. For example, inertial ordering exploits lift forces to arrange particles along a channel, allowing more than 80% of droplets to be loaded with one particle[6]. Alternatively, close-packed loading uses compliant particles that can be packed without clogging channels, arranging them into a regular lattice such that 94% of droplets can be loaded with one particle. Close packing is flexible with respect to flow rates, channel sizes and shapes, and utilizes biocompatible particles that are useful for downstream molecular biology[7,8].

Some applications of droplet microfluidics require encapsulating multiple particle types. For example, in growth assays, droplet gelation encases cells in hydrogel particles, keeping them separated while allowing small molecule diffusion for cell growth and characterization[9–11]. Additionally, in single cell genomics, gel particles containing cellular nucleic acids are co-encapsulated with particles containing barcode primers for RNA labeling[12]. However, current methods are unable to controllably load distinct particle types in droplets. Mixing particles together and using inertial or close packing methods, for instance, allows a large fraction of droplets to be loaded with two particles, but the particle types are randomly selected from the inputs, making many droplets unusable. For applications requiring multiple particles, a method that ensures that every droplet received an exact number of each particle type would be valuable.

In this paper, we introduce an approach to controllably load distinct particle types in droplets. Our approach merges separate close-packed streams in a microfluidic funnel, creating a single stream in which the particle types alternate, reminiscent of a zipper. By synchronizing the zipped stream with the droplet generation, a controlled number of each particle type is encapsulated per droplet. To showcase the utility of the device, we use it to perform single-cell DNA sequencing of cancer hotspots employing cell gel and barcode gel particles. Zipper modules form binary junctions and can be stacked to zip together multiple streams, allowing complex droplet encapsulations with a high degree of control.

2. Results and Discussion

2.1 Close-packed particles can be zipped into an interleaved stream

Several approaches have been described to control loading of multiple particles into droplets, including particle manipulation with surface acoustic waves or by droplet triggering upon particle detection. However, these methods require substantial user input and have a low throughput[13,14]. Because many droplet microfluidic protocols, such as single-cell methods, require high througput droplet generation with constant particle number, we focus our method around these goals - but sacrifice the capability to change the particle number in each droplet at will. Our approach to encapsulate multiple particles exploits the regularity of close-packed ordering to merge separate streams into one. Provided the particles are similar in size and injection rate, the streams interleave such that the particles alternate, reminiscent of a zipper mechanism (Fig. 1a). To encapsulate one of each particle type, the merged particle injection is synchronized with the droplet generation by adjusting flow rates, such that two particles enter for every droplet formed. To encapsulate more particles per droplet, particle injection can be increased, or droplet generation slowed. The result is a monodispersed emulsion in which most droplets contain the desired number of particles of each type (Fig. 1b). Non-equal ratios can be achieved by tuning particle injection rates.

To determine the periodicity of the zipping mechanism we record movies with a high-speed camera. We calculate the sum of grayscale values in sample boxes placed on the left and right side of the funnel at the interleaving point (Fig. 2a). Because the contact between adjacent particles appears bright (Fig. 1b), our probes detect spikes in grayscale intensity for the transition from one particle to the next (Supplementary movie 1). The two streams interact and order, so that we measure phase locked peaks with a half-period shift, indicating particle interleaving (Fig. 2c and Supplementary Fig. 1a, Supplementary movie 1). The time traces share a lowest major mode of ~100 Hz, the average particle injection frequency. Higher frequency modes are due to optical variations smaller than a particle diameter (downward peaks, Fig. 2a). Thus, the merged stream should have a lowest major mode of ~200 Hz, which indeed it does (Fig. 2d). The physical properties of the output stream are thus equivalent to each input stream at twice the flow rate. Consequently, particle zippers can be stacked in series to create complex repeating particle patterns. We observe flaws in the periodicity every ~30 particles, where two particles of the left channel insert instead of one. This indicates that the flow of the left stream is ~3% faster than the right. The result is that the phases of the time traces shift by a half particle period when this occurs. However, this has minimal impact on droplet encapsulation, since after the initial shift, which may result in a droplet containing two identical particle types, the phase of the interleaved stream no longer affects particle composition in the droplets (Supplementary Fig. 1a, Supplementary movie 1).

2.2 Zipped streams allow controlled co-encapsulation

To achieve controlled encapsulation using our stream zipper, we tune droplet formation frequency to half the particle reinjection frequency[7]. To assess the rate of successful co-encapsulation, we label the particles in the right channel with FITC (depicted green) and in the left channel with Cy5 (depicted blue). We collect and image the droplets using brightfield and fluorescence microscopy (Fig. 3a), observing monodispersed droplets in which ~90% contain two particles (Fig. 3a) and ~80% contain one of each particle type (Fig. 3b). Poisson loading at an average of two particles per droplet would yield just 13.5% containing one of each type, demonstrating that the particle zipper affords a significant improvement in encapsulation efficiency. Among droplets containing two particles, we observe Cy5 pairs but no FITC pairs, indicating slightly higher Cy5 particle injection rate.

2.3 Particle zipping allows efficient single cell DNA sequencing of cancer hotspots

Single-cell DNA sequencing allows characterization of genetically distinct tumor subpopulations relevant to disease progression and therapeutic resistance. Sequencing chromosomal DNA, however, is challenging because in its native state the genome is tightly packed as chromatin that hampers molecular biology. Harsh conditions are required to disrupt chromatin and make DNA accessible to amplification but are generally incompatible with amplification enzymes. To overcome this issue, a powerful strategy is to encapsulate cells in hydrogel particles that can be subjected to multiple bulk reactions to lyse cells, disrupt chromatin, and wash away reagents that would interfere with downstream genomic DNA amplification[4,15–17]. The resultant hydrogels can be paired with barcoding particles and reagents, to amplify and label target regions for sequencing. This requires co-encapsulation of cell particles with barcode particles, which can be efficiently achieved using our zipper.

To demonstrate this, we use the approach to sequence a mixture of K562 and CEM cells. We encase the cells in polyacrylamide particles by co-flowing an acrylamide solution with the cell suspension (Fig. 4a, left). After

polymerization, we break the emulsion and wash with detergent; this lyses the cells and disrupts chromatin, but high molecular weight genomic DNA remains trapped in the particles. We wash the particles again to remove detergent, then transfer into PCR buffer (Fig. 4a, Hydrogel particle A). In parallel, we prepare a separate batch of particles containing barcode sequences for DNA target labeling[1,4,18] (Fig. 4a, Hydrogel particle B). The particles are functionalized with barcode primers targeting 16 amplicons covering hotspots of genomic alterations in leukemic cells, and thus should yield divergent signals for these cell lines. Using our zipper device, we interleave and encapsulate the particle streams at a pairing rate of about 1000 cells per minute. Despite a size difference of ~15% between the two particle batches, we observe efficient pairing. We thermocycle the droplets, amplifying and barcoding the target loci for each cell, and prepare a sequencing library.

Sequencing reveals multiple recurrent polymorphisms, some pathological and some benign. This makes sense since the two cell lines are derived from different patients and thus harbor distinct genomic fingerprints. We use the detected chromosomal variants to calculate a pairwise distance between all cells and cluster the resultant distance matrix. Two major clusters are apparent (Fig. 4b) and the mean genomic signature within the clusters corresponds to the polymorphism detected in a bulk sample for the two cell lines, indicating that the two-gel merging workflow identifies chromosomal signatures in single-cells with high sensitivity.

3. Conclusion

Droplet microfluidic single cell analysis allows deconvolution of cellular heterogeneity inherent in biological samples, and novel protocols continue to be developed for this purpose. These approaches exploit the ability of droplet microfluidics to generate millions of individual reaction vessels. However, manipulating droplet contents is challenging because droplets cannot be subjected to bulk washes without destroying them. Consequently, most workflows strictly adhere to a single encapsulation step, limiting the reactions that can be performed. Immobilizing reactants in hydrogel particles is a flexible way to achieve segregation while allowing multiple bulk processing steps; thus, workflows exploiting hydrogel particles are becoming common. In many instances, it is necessary to further process hydrogels in microfluidic devices and, often, to co-encapsulate one batch of hydrogels with another. Our particle zipper thus addresses a key technical gap, allowing distinct hydrogel streams to be zipped into a uniform alternating stream that allows precision loading of droplets with exact types of particles. Moreover, the output of zipped streams is identical in flow and geometric properties to input streams, allowing multiple zippers to operate in one junction, or a cascade of pairwise zippers to generate a final stream with a repeating sequence of different particle types. This should allow merging of multiple streams to uniformly load droplets with complex particle combinations a feat that, until now, has relied on random loading and yielded tiny fractions of correctly loaded droplets.

Zippers are attractive because they are simple to fabricate and operate in microfluidic devices. However, they constrain the usable particles by requiring close packed input streams to operate successfully; hence, the particles need to be compliant and match the inlet dimensions[7]. For practical purposes, small size discrepancies, for example stemming from batch to batch variability, do not prevent successful particle pairing. For particles with dissimilar diameter, the close packing requirement can be satisfied by designing an asymmetric zipper with inlet aspect ratios matching the two bead streams.

While particle zipping should be useful for any application involving at least two different hydrogel types, a particularly valuable application is single cell epigenomic characterization. Epigenomic sequencing often requires treating genomic DNA with multiple reagents to prepare it for sequencing, and zipping can combine pre-treated particles with barcode particles for labeling, providing flexibility in epigenome processing.

4. Methods

4.1 Device fabrication.

We used standard photolithography to make structures on a 3-inch silicon waver with SU-8 3050 photoresist (MicroChem, Westborough, MA, USA). PDMS prepolymer and curing agent (Sylgard 184 silicone elastomer kit) were mixed at a ratio 1:10, de-gassed in a vacuum chamber, poured over the mold, de-gassed until no more bubbles were visible and baked at 65°C over night. PDMS replica was removed from the mold, inlets and outlets punched with a custom made 0.75 mm biopsy puncher and plasma bonded to glass slides (75×50×1 mm, 12-550C, Fisher Scientific) by treating with oxygen plasma for 60 s at 1 mbar (PDC-001, Harrick Plasma). Device was baked at 150°C for 1 hour to complete bonding, treated with Aquapel (PPG Industries) with a contact time of about 5 minutes and purged with air. Remaining Aquapel was evaporated by baking device for 1 h at 65°C.

4.2 Cell culture

Acute lymphoblastic leukemia cells (CEM, ATCC CRL-2265) were cultured in RPMI Media 1640 with 10% Fetal Bovine Serum, Penicillina and Streptomycin at 37°C and 5% CO_2. Chronic myelogenous leukemia cells (K562, ATCC CRL-2265) were cultured in Iscove's Modified Dulbecco's Medium with the same additives and under the same conditions as above.

4.3 Hydrogel particle synthesis

Polyacrylamide hydrogels for FAM and Cy5 staining and custom split pool barcoding were made similar to a previous description[10] with a simple microfluidic drop maker. The device was scaled down to a 30 μm nozzle with and 33 μm device height to make droplets of 45 μm diameter. A solution of 6% acrylamide and 0.15% bis-acrylamide (40:1 acrylamide : bis-acrylamide), 0.3% ammonium persulphate, 48 mM Tris-HCl pH 8.0 and 0.1x TBSET (20 mM Tris-HCl pH 8.0, 274 mM NaCl, 5.4 mM KCl, 20 mM EDTA, 0.2 % Trition X100) was used as dispersed phase (1000 μl/h) and the continuous phase consisted of HFE-75000 with 2% (w/v) PEG-PFPE amphiphilic block copolymer[20] and 0.4 % N,N,N',N'-tetramethylethylenediamine (ThermoFisher) (1236 μl/h). Droplets were incubated for 4 h at room temperature to allow for gel polymerization and particles were recovered by adding 20% 1H,1H,2H,2H-perfluoro-1-octanol in HFE 7500, vortexing, centrifugation and removing the oil phase with a pipette. Particles were washed 3 times in TEBST and 3 times in TET (10 mM Tris-HCl pH 8.0, 10 mM EDTA, 0.1 % Tween-20) also serving as storage buffer. Particles had an average diameter of 53 μm with a coefficient of variation <10%.

Cells were encapsulated in polyacrylamide gels by coflowing a cell suspension with the gel precursor mixture. The cell suspension was made by mixing K562 and CEM cells at a 1:1 ratio and resuspended at 2.2 million cells per ml in Phosphate Buffered Saline with 0.1 mg/ml BSA and 605 mM sorbitol (to match the cell density). Gel precursor mix was prepared as above at 2x concentration and substituting 0.3% bis-acrylamide with 0.51% w/v N,N′-Bis(acryloyl)cystamine (Sigma, CAS Number 60984-57-8) and 1% w/v sodium dodecyl sulfate (SDS) was added. Cell suspension and gel precursor were co-flowed at a 1:1 ratio (each at 750 μl/h) and combined with the oil mix from above (1800 μl/h) on a bubble-triggered device[21]. After demulsification and TEBST washes particles were incubated in TET + 1% w/v SDS at 65°C for 30 min, followed by 6 wash cycles in TET and stored in TET at 4°C until use. Final particles were monodispersed and had an average diameter of 61.5 μm. The cell encapsulation rate was ~0.185 cells per particle, determined by staining the encapsulated chromosomal DNA with SYBR Green I and counting with a fluorescence microscope (EVOS Cell Imaging System, Thermo Fisher Scientific). All particles were strained through a 70 μm cell strainer (Falcon) prior to use to remove aggregates and dust particles which can cause clogging.

4.4 Particle reinjection analysis

Particles were labeled with fluorophores by hybridizing DNA oligomers modified with FAM or Cy5 (FAM-AAGTTCAGCAGGAATCGGCATTT or Cy5-AAGTTCAGCAGGAATCGGCATTT) to the constant region used for split-pool barcoding. Particles were resuspended in solution A (10 mM Tris-HCl pH 8.0, 40 mM NaCl, 3.75 % (v/v) Tween-20, 2.5 mM $MgCl_2$, 2.5 % (v/v) Glycerol, 0.625 mg/ml BSA) and reinjected at 60 μl/h each. The particle stream was co-flowed with solution A at 180 μl/h and HFE-7500 with 2% (w/v) PEG-PFPE at 300 μl/h. For particle pairing periodicity high speed movies with a Phantom V7 camera at 10,000 frames per second were recorded and the average gray scale over the line positions indicated in figure 2a minus the global average greyscale over the entire image was extracted. The global average gray scale value oscillates with a frequency of 120 Hz (supplementary figure 1b) which is twice the carrier frequency of the United States, and would confound the droplet signal without this correction. Discrete Fast Fourier Transform of the full-length time trace (supplementary figure 1a) multiplied by the Hann Window function was calculated with the numpy (v1.1.2.0) fast Fourier transform and Hanning window routines.

4.5 Cell genotyping

Cell gel particles were resuspended in solution B (10 mM Tris-HCl pH 8.0, 40 mM NaCl, 3.75 % (v/v) Tween-20, 2.5 mM $MgCl_2$, 0.8 M propane-1,2-diol, 0.625 mg/ml BSA)(0.1% Tween-20 in the bead buffers helps preventing clogging, here we use a higher concentration to stabilize the emulsion during PCR), 16 reverse primers (supplementary table 1) were added at a final concentration of 0.142 μM each; particles were close packed to an approximate solid fraction range of 75-90% (v/v) and reinjected at 70 μl/h. Barcode gel particles in solution A, close packed and reinjected at 50 μl/h to account for the difference in size (53 μm and 61.5 μm in diameter) and match the reinjection frequency of the cell particles. The zipped particle stream was co-flowed with PCR mix (1.67x NEBNext Ultra II Q5 Master Mix (M0544S), 0.025 U/μl NEB User II (M5508S), 3.33 mM DTT, 0.25 mg/ml BSA, 0.8 M propane-1,2-diol) at 180 μl/h and HFE-7500 with 2% (w/v) PEG-PFPE and droplets fraction collected with a 2 min interval once flow stabilized to profile 1500-2000 cells. Excess oil was removed from collected fractions and replaced with FC-40 oil (Sigma) with 5% (w/v) PEG-PFPE and the emulsion thermocycled with all ramp speeds set to 1°C/s: 30°C, 30 min, 95°C, 3 min; 95°C, 15 s; 72°C, 15 s; 62.5°C, 2 min; 72°C, 30 s; repeat total 15 times; 72°C, 2 min; 12°C hold.

The thermocycled emulsion was overlaid with 5 volumes of 1x ExoI (NEB, M0293S) solution to digest unused primers and demulsified with 1H,1H,2H,2H-perfluoro-1-octanol and incubated for 1 h at room temperature. Polyacrylamide particles were pelleted and supernatant purified with 0.75 x AMPure beads (Beckmann Coulter). Eluted amplicons were

subjected to library PCR with custom P5 and P7 primer (supplementary table 1) and sequenced on a MiSeq v2 300 cycles kit (Illumina) with custom forward primer and built in reverse primer. Bulk cell sample libraries were prepared by using a corresponding set of forward (without barcodes) and reverse primers to amplify the same genomic loci as in droplets from extracted DNA from CEM and K562 cells. Library preparation was then done analogously.

4.6 Data evaluation

Fasta files for read 1 and read 2 were demultiplexed into barcode groups by a custom python script and cutadapt (v2.4)[22]. Barcode groups from valid cells were identified by inspecting the barcode rank plot versus number of associated reads and selected by the knee method, reads were aligned, and variants called all as previously described[23] which yielded 1620 cells. The result is a matrix of cells by variants, where each row represents a single cell, each row a genomic variant and the matrix elements are categorial variables denoting: 0, wild type; 1, heterozygous; 2, alternate and 3, no call. To cluster cells the variant call matrix was converted to a binary matrix were 0 denotes wild type or no call and 1 alternate or heterozygous. The Jaccard similarity between all cells was calculated and visualized in two dimensions by Uniform Manifold Approximation and Projection (UMAP) using the python UMAP library (v0.3.9)[24]. To order cells by similarity, heterozygous and alternate calls were used and cells clustered with the scipy (v1.3.1) cluster hierarchy method using Ward's minimum variance criterion. Genomic variants were selected for visualization by filtering all variants that had more than 70% dropout or more than 90% wild type call to retain informative loci only. Remaining variants were inspected for non-biological variability caused by inconsistent alignments of variants to adjacent nucleotide positions which were manually removed.

Conflicts of interest

The authors declare that they have no competing financial interests.

Acknowledgment

We thank members of the Abate lab, in particular Benjamin Demaree, Christian A. Siltanen, Leqian Liu and Samuel C. Kim for discussions and advice and Sarah Pyle for helping with the visualizations. This work was supported by the Chan Zuckerberg Biohub, the National Institutes of Health (NIH) (Grant No. R01-EB019453-01, R01-HG008978 and DP2-AR068129-01), the National Science Foundation CAREER Award (Award No. DBI-1253293); C.L.D is supported by the Swiss National Science Foundation (SNF) (Grants No. 175086, No. 183853).

References

1 A. M. Klein, L. Mazutis, I. Akartuna, N. Tallapragada, A. Veres, V. Li, L. Peshkin, D. A. Weitz and M. W. Kirschner, Droplet Barcoding for Single-Cell Transcriptomics Applied to Embryonic Stem Cells, *Cell*, 2015, **161**, 1187–1201.

2 E. Z. Macosko, A. Basu, R. Satija, J. Nemesh, K. Shekhar, M. Goldman, I. Tirosh, A. R. Bialas, N. Kamitaki, E. M. Martersteck, J. J. Trombetta, D. A. Weitz, J. R. Sanes, A. K. Shalek, A. Regev and S. A. McCarroll, Highly Parallel Genome-wide Expression Profiling of Individual Cells Using Nanoliter Droplets, *Cell*, 2015, **161**, 1202–1214.

3 P. Shahi, S. C. Kim, J. R. Haliburton, Z. J. Gartner and A. R. Abate, Abseq: Ultrahigh-throughput single cell protein profiling with droplet microfluidic barcoding, *Sci. Rep.*, 2017, **7**, 44447.

4 M. Pellegrino, A. Sciambi, S. Treusch, R. Durruthy-Durruthy, K. Gokhale, J. Jacob, T. X. Chen, J. A. Geis, W. Oldham, J. Matthews, H. Kantarjian, P. A. Futreal, K. Patel, K. W. Jones, K. Takahashi and D. J. Eastburn, High-throughput single-cell DNA sequencing of acute myeloid leukemia tumors with droplet microfluidics, *Genome Res.*, 2018, **28**, 1345–1352.

5 L. Mazutis, J. Gilbert, W. L. Ung, D. A. Weitz, A. D. Griffiths and J. A. Heyman, Single-cell analysis and sorting using droplet-based microfluidics, *Nat. Protoc.*, 2013, **8**, 54–56.

6 J. F. Edd, D. Di Carlo, K. J. Humphry, S. Köster, D. Irimia, D. A. Weitz and M. Toner, Controlled encapsulation of single-cells into monodisperse picolitre drops, *Lab Chip*, 2008, **8**, 1262–1264.

7 A. R. Abate, C.-H. Chen, J. J. Agresti and D. A. Weitz, Beating Poisson encapsulation statistics using close-packed ordering, *Lab Chip*, 2009, **9**, 2628.

8 I. C. Clark and A. R. Abate, Microfluidic bead encapsulation above 20 kHz with triggered drop formation, *Lab Chip*, 2018, **18**, 3598–3605.

9 W.-G. Koh and M. V. Pishko, Fabrication of cell-containing hydrogel microstructures inside microfluidic devices that can be used as cell-based biosensors, *Anal. Bioanal. Chem.*, 2006, **385**, 1389–1397.

10 W. H. Tan and S. Takeuchi, Monodisperse alginate hydrogel microbeads for cell encapsulation, *Adv. Mater.*, 2007, **19**, 2696–2701.

11 Y. Tsuda, Y. Morimoto and S. Takeuchi, Monodisperse Cell-Encapsulating Peptide Microgel Beads for 3D Cell Culture, *Langmuir*, 2010, **26**, 2645–2649.

12 L. Liu, C. K. Dalal, B. M. Heineike and A. R. Abate, High throughput gene expression profiling of yeast colonies with microgel-culture Drop-seq, *Lab Chip*, 2019, **19**, 1838–1849.

13 D. J. Collins, T. Alan, K. Helmerson and A. Neild, Surface acoustic waves for on-demand production of picoliter droplets and particle encapsulation, *Lab Chip*, 2013, **13**, 3225.

14 D. J. Collins, A. Neild, A. deMello, A.-Q. Liu and Y. Ai, The Poisson distribution and beyond: methods for microfluidic droplet production and single cell encapsulation, *Lab Chip*, 2015, **15**, 3439–3459.

15 M. V. Tamminen and M. P. J. Virta, Single gene-based distinction of individual microbial genomes from a mixed population of microbial cells, *Front. Microbiol.*, 2015, **6**, 195.

16 L. Xu, I. L. Brito, E. J. Alm and P. C. Blainey, Virtual microfluidics for digital quantification and single-cell sequencing, *Nat. Methods*, 2016, **13**, 759–762.

17 F. Lan, B. Demaree, N. Ahmed and A. R. Abate, Single-cell genome sequencing at ultra-high-throughput with microfluidic droplet barcoding, *Nat. Biotechnol.*, 2017, 1–10.

18 R. Zilionis, J. Nainys, A. Veres, V. Savova, D. Zemmour, A. M. Klein and L. Mazutis, Single-cell barcoding and sequencing using droplet microfluidics, *Nat. Protoc.*, 2016, **12**, 44–73.

19 D. J. Collins, A. Neild, A. deMello, A.-Q. Liu and Y. Ai, The Poisson distribution and beyond: methods for microfluidic droplet production and single cell encapsulation, *Lab Chip*, 2015, **15**, 3439–3459.

20 C. Holtze, A. C. Rowat, J. J. Agresti, J. B. Hutchison, F. E. Angilè, C. H. J. Schmitz, S. Köster, H. Duan, K. J. Humphry, R. A. Scanga, J. S. Johnson, D. Pisignano and D. A. Weitz, Biocompatible surfactants for water-in-fluorocarbon emulsions, *Lab Chip*, 2008, **8**, 1632.

21 Z. Yan, I. C. Clark and A. R. Abate, Rapid Encapsulation of Cell and Polymer Solutions with Bubble-Triggered Droplet Generation, *Macromol. Chem. Phys.*, 2017, **218**, 1600297.

22 M. Martin, Cutadapt removes adapter sequences from high-throughput sequencing reads, *EMBnet.journal*, 2011, **17**, 5–7.

23 B. Demaree, C. L. Delley, H. N. Vasudevan, C. A. C. Peretz, D. Ruff, C. C. Smith and A. R. Abate, Joint profiling of proteins and DNA in single cells reveals extensive proteogenomic decoupling in leukemia, *bioRxiv*, 2020, 2020.02.26.967133.

24 L. McInnes, J. Healy and J. Melville, UMAP: Uniform Manifold Approximation and Projection for Dimension Reduction.

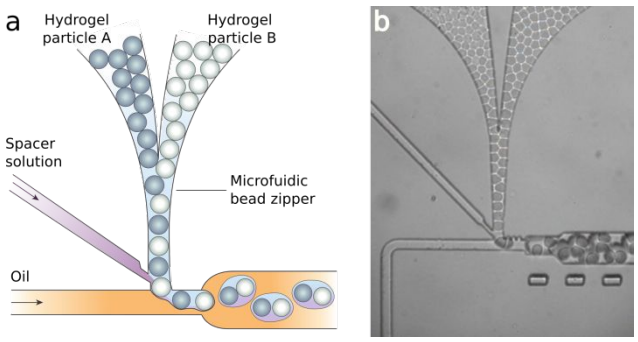

Fig. 1, Microfluidic particle zipper mechanism: a) Interleaving two close-packed hydrogel particle streams (grey and blue) in a microfluidic zipper enables deterministic co-encapsulation in droplets. b) Transmission light microscope image of the zipper device during operation. The particles have a diameter of ~50 μm.

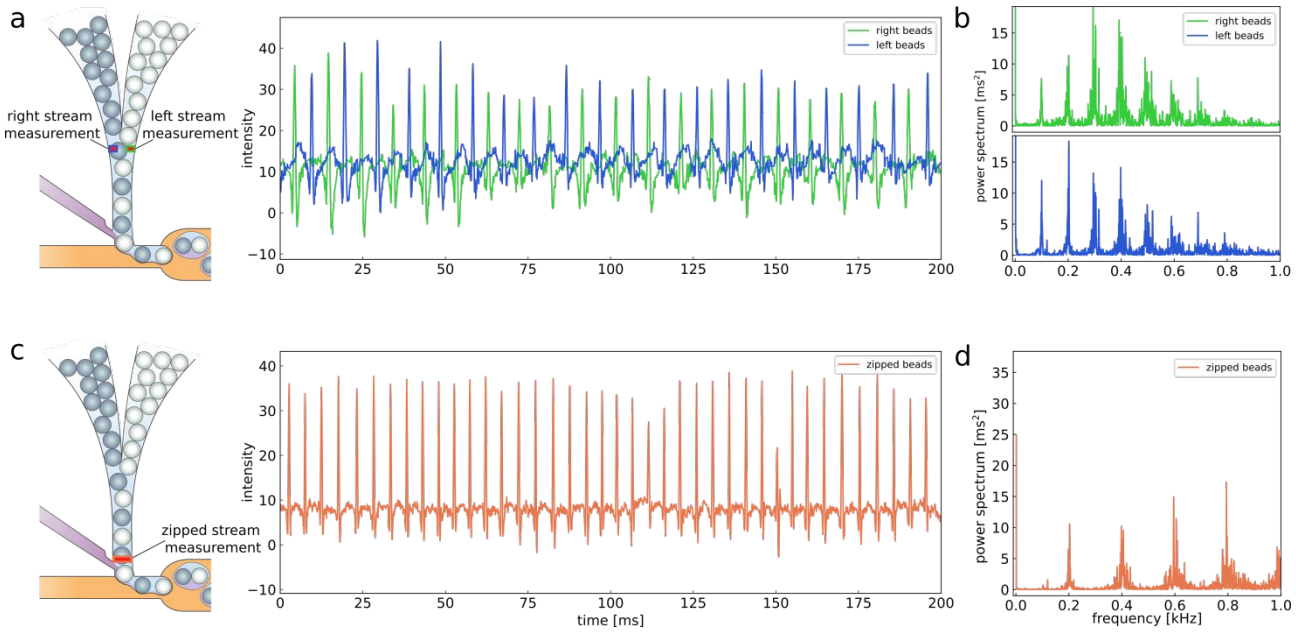

Fig 2, Particle zipping is ordered and periodic: a) Left side, cartoon indicating the positions for the gel particle passage measurement. Grey scale values of corresponding pixels are measured for each frame in the encapsulation movie (supplemental movie 1). Right side, representative section of the time trace series for the demarcated positions in a). b) Discrete Fourier Transform power spectrum for the full-length time traces in a). c) and d) same as a) and b) for the particle stream after zipping the streams.

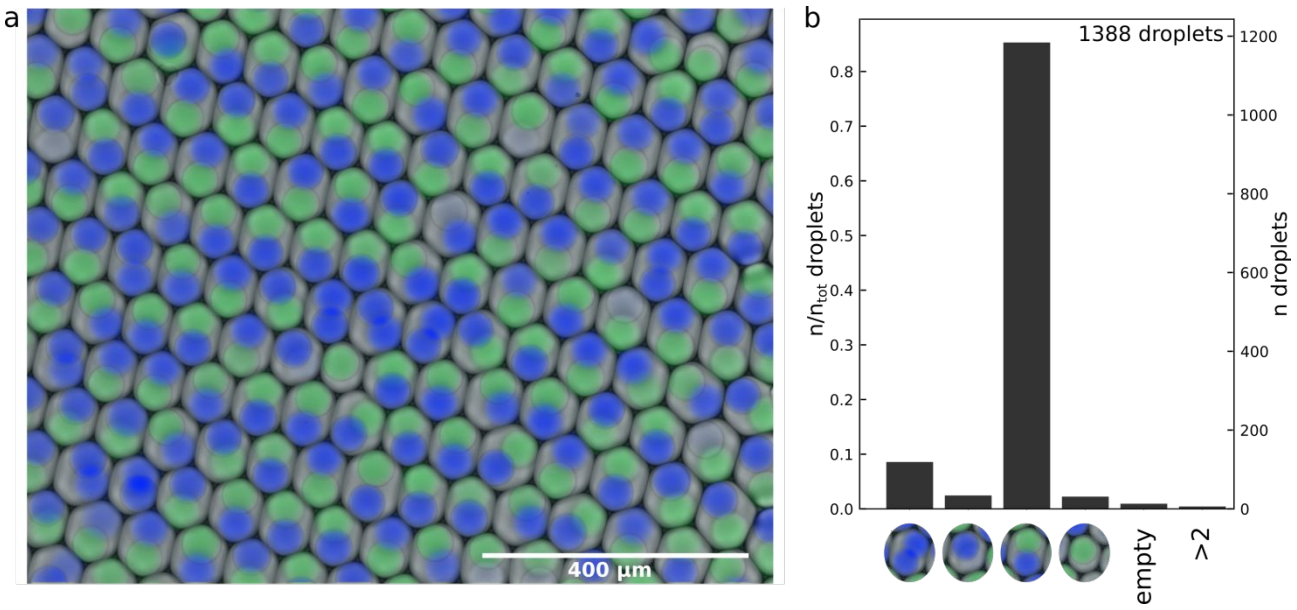

Fig 3, Particle zipping allows controlled loading of droplets with distinct particles: a) Microscope image of droplets collected from the pairing device. The transmission light image is overlaid with the FAM fluorescence image (false colored green) and Cy5 fluorescence image (false colored blue). b) Frequency of droplet loading compositions. Droplets with >2 gels are binned together.

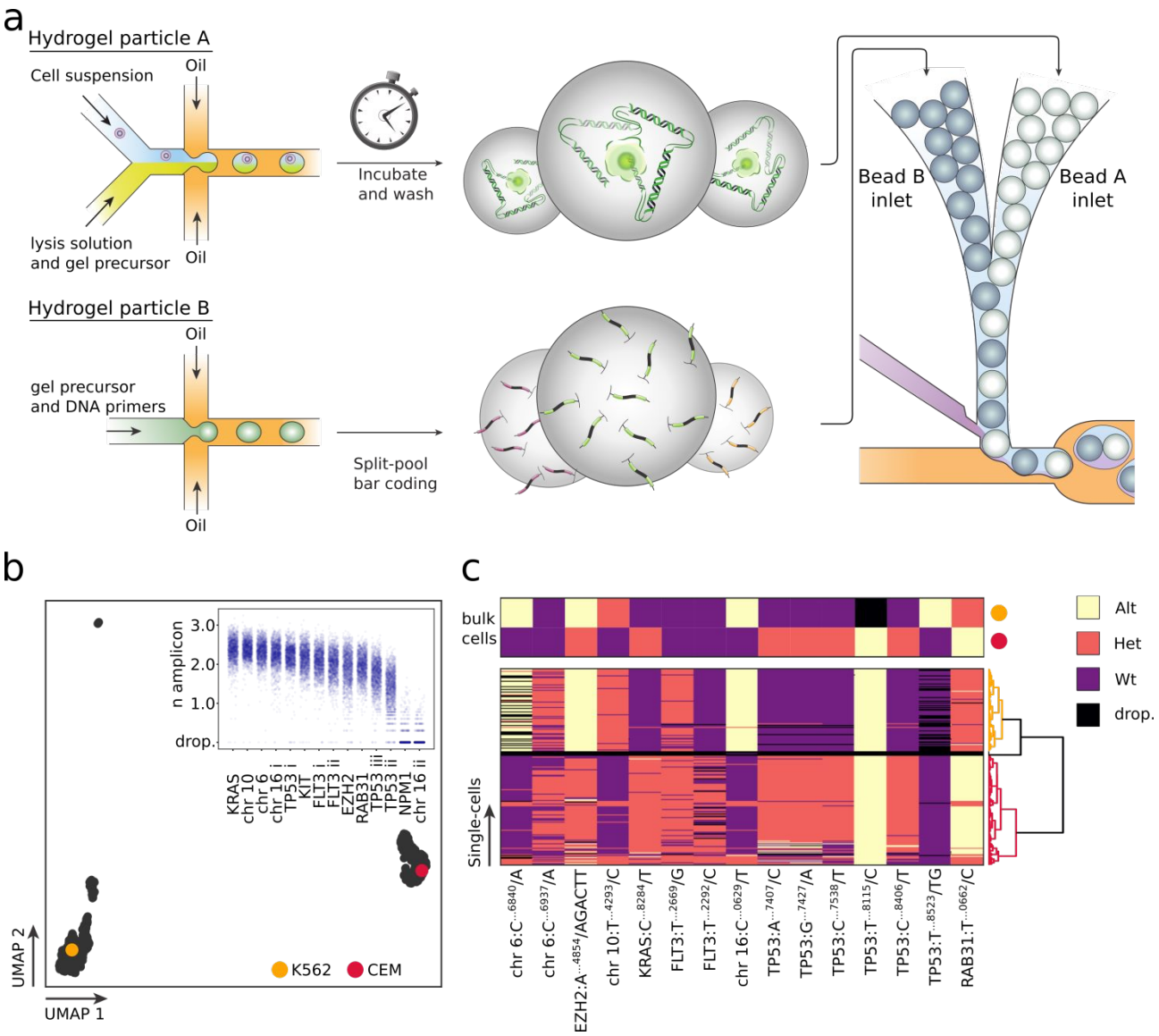

Fig 4, Zipping cell and barcode particles allows efficient single cell genotyping a) Single cell genotyping workflow. Cells are encapsulated with acrylamide and SDS to form hydrogels containing the genome of the cells. Barcode particles with a 16-plex panel of forward primers are paired with cell particles and PCR reagents on the microfluidic particle zipper. Droplet PCR is performed off chip to generate barcoded amplicons of the 16 targeted genomic loci. b) Two cell line experiment: genomic variants are called from the barcoded amplicons, assigned to single cells based on barcodes and the Jaccard similarity between cells calculated (methods). UMAP embedding reveals two populations, clustering around the bulk variant call profile of the two cell lines (colored dots). Outlier population in the top left corner are barcode groups without valid variant calls. Inlet shows detected number of amplicons per barcode group and amplicon as log 10 counts. Two out of 16 targets did not amplify in any cell. c) Differential variant call profile measured for the bulk (top) and single-cell (bottom) samples across the 16 amplicons. Single cells are ordered by hierarchical clustering using Ward's minimum variance criterion. Colors indicate cell type assignment (red and yellow) and barcode group without valid variant calls (black).

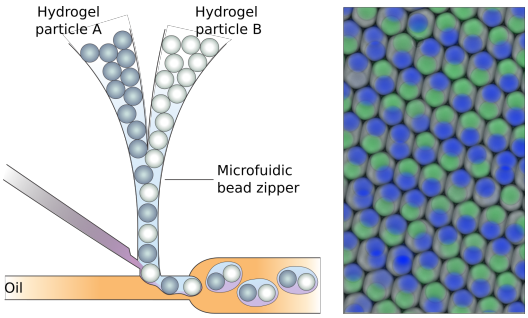

We describe a microflidic particle zipper which enables hydrogel bead pairing at high throughput for single-cell genomic applications.